HHS Public Access

Author manuscript

J Mater Chem B Mater Biol Med. Author manuscript; available in PMC 2018 January 05.

Published in final edited form as:

J Mater Chem B Mater Biol Med. 2017 ; 5(6): 1195–1204. doi:10.1039/C6TB02819E.

Bioactive mono-dispersed nanospheres with long-term antibacterial effects for endodontic sealing

Xiaogang Cheng[a,b], **Tiejun Qu**[a], **Chi Ma**[b], **Doudou Xiang**[a], **Qing Yu**[a,*], and **Xiaohua Liu**[b,*]

[a]State Key Laboratory of Military Stomatology & National Clinical Research Center for Oral Diseases & Shaanxi Key Laboratory of Stomatology, Department of Operative Dentistry and Endodontics, School of Stomatology, The Fourth Military Medical University, 710032, Shaanxi, China

[b]Biomedical Sciences Department, Texas A&M University College of Dentistry, Dallas, TX, 75246, USA

Abstract

Endodontic sealers with antibacterial capability play an important role in preventing reinfection of an endodontically treated root canal and improving the long-term success of root canal treatment. However, current endodontic sealers rapidly lose their antibacterial properties after fixation. In this work, we designed and synthesized quaternized mono-dispersed bioactive nanospheres as a potential substrate for the development of a long-term antibacterial endodontic sealer with excellent cytocompatibility and biocompatibility. First, mono-dispersed silica-based bioactive glass nanospheres (SBG-NS) were prepared via a modified sol-gel process. Next, a series of quaternary ammonium methacrylate salts (QAMs) with broad antibacterial spectra were synthesized and grafted onto the surfaces of the SBG-NS via a two-step coupling approach. The antibacterial effect of the quaternary ammonium polymethacrylate (QAPM)-containing SBG-NS (SBG-QAPM) against persistent microorganisms associated with infected root canals was evaluated using a direct contact test. Evaluations of the SBG-QAPM cytocompatibility and biocompatibility were performed using LIVE/DEAD staining, 3-(4, 5-dimethylthiazol-2-yl)-2, 5-diphenyl-2, 5-tetrazoliumbromide (MTT) assay, and a calvarial implantation model. The results showed that the SBG-QAPMs had the strongest long-term antibacterial effect against the *Enterococcus faecalis*, *Streptococcus mutans*, and *Streptococcus sanguis* during the study period, the best cytocompatibility, and the lowest systemic inflammation compared to three commercial products: ProRoot MTA, Endomethasone C, and AH Plus. In addition, the SBG-QAPMs showed excellent stability in aqueous solution. This work indicates that the SBG-QAPMs are promising substrates for the development of long-term antibacterial endodontic sealers.

xliu@tamhsc.edu; Fax: +1 214-874-4538; Tel: +1 214-370-7007.

Disclosure statement

All the authors declare there is no conflict of interest related to the work.

1 Introduction

Pulpal and periapical diseases are among the most common oral diseases causing considerable discomfort, orofacial pain, and ultimately tooth loss.[1] These diseases cause physical and mental suffering and compromise a patient's quality of life. In addition, they also act as a reservoir of infection for systemic diseases such as bacterial endocarditis and cardiovascular diseases.[2,3] Presently, root canal therapy is the most widely used procedure to treat pulpal and periapical diseases with severe infection. During root canal treatment, the infected tissues are removed, and the root canal system is shaped, disinfected, and sealed with a core bio-inert material (e.g., gutta percha) combined with an endodontic sealer.[4] The elimination of infection within the canal is crucial for the success of a root canal treatment, which is currently carried out through a variety of chemo-mechanical techniques.[5,6] Due to the complicated anatomical structure of the tooth root, it is well known that the complete eradication of the bacteria in the canal and dentin tubules is virtually impossible, regardless of instrumentation and irrigation procedures.[7,8] The residual bacteria can cause reinfection, leading to the failure of the endodontic treatment. Therefore, as the final step in a root canal treatment, it is desirable for the endodontic sealer to exhibit an antibacterial effect to eliminate or inhibit the growth of residual bacteria that are untouched by the chemo-mechanical procedure.

Current commercial endodontic sealers have a certain degree of short-term antibacterial activity, which is due to the release of antibacterial ingredients in the sealer prior to their fixation. For example, zinc-oxide-eugenol-based (ZnOE-based) sealers release free eugenol, and epoxy-amine-resin-based sealers release formaldehyde and bisphenol-A diglycidyl ether during the curing process.[9,10] It was reported that those sealers lose their antibacterial effect in hours or days after fixation because of the loss of the antibacterial components.[10,11] While studies also showed that the ZnOE-based and epoxy-amine-resin-based sealers can present a certain antibacterial effect up to 30 days and even longer,[12–14] their cytotoxicity should be taken into consideration.[15] The released antibacterial components (e.g., eugenol and formaldehyde) could trigger moderate to severe cytotoxicity to cells and periapical tissues.[16,17] In addition, the loss of the antibacterial components has led to the shrinkage of the sealer, which compromises the sealing effect.[18,19] A number of efforts have been made to improve the antibacterial effect of the endodontic sealers currently used in clinics,[5,12,20,21] and the most widely used method is the addition of extra antibacterial ingredients in the sealer. For example, endodontic sealers Kerr Pulp Canal Sealer EWT, AH Plus, and RealSeal SE were mixed with antibiotics such as amoxicillin and metronidazole.[22–24] Those freshly mixed samples had a better antibacterial effect than their unmodified counterparts. However, they showed no superiority in the long term, compared to the unmodified controls. Endodontic sealers mixed or coated with cationic nanoparticles and silver ions were also developed to provide antibacterial activity.[11,25] Similarly, those materials showed a short-term antibacterial effect and a compromised biocompatibility. Silicon-containing root canal sealers have been developed due to their favorable biocompatibility. However, they had a weak antibacterial effect similar to that of calcium-hydroxide-based sealers.[26–28] To date, the development of a root canal sealer with long-term antibacterial activity and good biocompatibility remains a challenge.

In this work, we synthesized a novel type of substrate for the development of long-term antibacterial endodontic sealers via grafting quaternary ammonium polymethacrylate salts (QAPMs) on the surface of mono-dispersed silica-based bioactive glass nanospheres (SBG-NS). We selected silica-based bioactive glass as the core sealing material because of its excellent biocompatibility.[16] QAPM is a type of quaternary ammonium compounds that are cationic antimicrobials and kill a broad spectra of both gram-positive and gram-negative bacteria.[17] We first used a sol-gel process to prepare mono-dispersed SBG-NS. Next, we synthesized a series of quaternary ammonium methacrylate salts (QAMs) and grafted them onto the surface of the SBG-NS via a coupling reaction and a free radical polymerization process (Scheme 1). We hypothesized that this QAPM-containing SBG-NS (SBG-QAPM) would present a long-term antibacterial effect as well as excellent cytocompatibility and biocompatibility. In addition, the nano-sized SBG-NS can readily penetrate into dentinal tubules and entomb any residual bacteria within the tubules, therefore providing another layer of protection from reinfection.

In this study, we first synthesized and characterized this novel type of SBG-QAPMs. Next, the antibacterial effect of the SBG-QAPMs against persistent microorganisms associated with infected root canals was compared with three representative commercial products (ProRoot MTA, Endomethasone C, and AH Plus) using a direct contact test (DCT). Finally, evaluations of the cytocompatibility and biocompatibility of the SBG-QAPMs were performed using LIVE/DEAD staining and 3-(4, 5-dimethylthiazol-2-yl)-2, 5-diphenyl-2, 5-tetrazoliumbromide (MTT) assay in vitro and calvarial implantation *in vivo*.

2 Experimental Section

2.1 Materials

Cetyltrimethylammonium bromide (CTAB, ≥ 99%), 28% ammonium hydroxide solution, tetraethyl orthosilicate (TEOS, ≥ 99%), triethyl phosphate (TEP, ≥ 98%), tetrahydrate calcium nitrate (CN, ≥ 99%), ethyl alcohol (ethanol, ACS reagent, ≥ 99.5%), 3-(trimethoxysilyl) propyl methacrylate (KH-570, ≥ 98%), toluene (anhydrous, ≥ 99.8%), 2-(dimethylamino) ethyl methacrylate (DMAEMA, ≥ 98%), 1-bromopropane (BP, ≥ 99%), 1-bromononane (BN, ≥ 98%), 1-bromohexadecane (BHD, ≥ 97%), 1-bromooctadecane (BOD, ≥ 97%), 1-butanol (anhydrous, ≥ 99.8%), benzoyl peroxide (BPO, 75%, remainder water), and distilled water (DW, Growcells) were all purchased from Sigma-Aldrich and used without further purification.

2.2 Synthesis of SBG-NS

SBG-NS were synthesized using a CTAB-assistant sol-gel process. CTAB was used as a catalyst and template agent in the reaction. First, CTAB (400 mg) was dissolved in 160 ml of DW and 6 ml of 28% ammonia to form a solution. The pre-dissolved inorganic sources (124 μL of TEP in 1 ml of ethanol, 520 mg of CN in 1 ml of DW, and 2.6 ml of TEOS in 1 ml of ethanol) were sequentially added dropwise to the CTAB solution at intervals of 30 min. The mixture was stirred magnetically for 24 h at room temperature. During the stirring process, the clear solution gradually became opaque and formed white precipitations (SBG-NS gels). The SBG-NS gels were collected by centrifugation (10, 000 × g) and rinsed three times with

ethanol and DW. After air drying at room temperature for 1 week, the templates and organic components in the SBG-NS gels were removed by calcination at 600°C for 5 h at a ramping rate of 1°C/min. The final SBG-NS appeared as fine white powders.

2.3 Coupling KH-570 to the surface of SBG-NS

SBG-NS (5 g) were dispersed in 50 ml of anhydrous toluene, and KH-570 (10 ml) was added to the SBG-NS suspension. The reaction was conducted under magnetic stirring (350 × g) in a silicone oil bath at 130°C for 1, 4, 24, or 48 h. The mixture was collected by centrifugation (10,000 × g) and extracted with ethanol for 8 h to remove the residual KH-570. The final product was rinsed three times with DW and freeze-dried for 48 h.

2.4 Synthesis of QAMs

A serial of QAMs with different lengths of alkyl chains were synthesized via the addition reaction of tertiary amines with organo-halides. Here we use propyldimethyl ammonium ethyl methacrylate bromide (PAEMB) as an example to describe the synthesis process. DMAEMA (10 mmol), BP (10 mmol), and ethanol (3 ml) were added to a vial equipped with a magnetic stirring bar. The vial was capped and stirred (350 × g) at 70°C for 24 h. After removal of the solvent by evaporation, a clear viscous product was obtained. The product was recrystallized three times with ethanol and freeze-dried for 48 h. The final product was denoted as PAEMB [alkyl chain length CL= 3]. Similarly, the other three QAMs, which are nonyldimethyl ammonium ethyl methacrylate bromide (NAEMB, CL=9), hexadecyldimethyl ammonium ethyl methacrylate bromide (HAEMB, CL=16), and octadecyldimethyl ammonium ethyl methacrylate bromide (OAEMB, CL=18), were synthesized using the same process.

2.5 Synthesis of SBG-QAPMs

The KH-570-modified SBG-NS (SBG-NS/KH-570, 5 g) was dispersed in 50 ml of 1-butanol in a three-neck round bottom flask (250 ml). The flask was equipped with a magnetic stir bar and a reflux condenser. After purging with nitrogen for 30 min, QAM (5 g) and BPO (50 mg) were added to the flask using a syringe. The reaction was allowed to proceed at 80°C under magnetic stirring (350 × g) and nitrogen protection conditions. After 24 h, the raw product was collected, rinsed with ethanol and DW for three times, and freeze-dried for 48 h. Four kinds of the QAMs were grafted to the SBG-NS/KH-570, and they were abbreviated as SBG-PA, SBG-NA, SBG-HA, and SBG-OA. They were stored in a desiccator for future use.

2.6 Characterization of SBG-NS, QAMs, and SBG-QAPMs

2.6.1 Scanning electron microscopy (SEM) evaluation—The SBG-NS samples (n = 3) were dispersed in ethanol, mounted onto the surface of a silicon wafer, and dried in a lyophilizer (ES-2030, Hitachi, Japan). The dried SBG-NS samples were gold-coated for 180s using a sputter coater (SPI-Module Sputter Coater Unit, SPI Supplies/Structure Probe, Inc.), and observed them by SEM (S-4800, Hitachi, Japan). During the gold-coating process, the gas pressure was kept at 50 mTorr, and the current was held at 20 mA. For image acquisition, each specimen was divided into four quadrants, and three microscopic fields

were recorded randomly at 20,000 × magnification in each quadrant. The size and distribution of the SBG-NS were calculated based on the SEM images using NIH freeware ImageJ (http://rsb.info.nih.gov/ij/index.html). For each SBG-NS and SBG-QAPM, the diameter was determined by averaging its two perpendicular diameters. The diameters of all SBG-NS and SBG-QAPMs from the SEM images (n = 3×4×3 = 36) were recorded and then averaged.

2.6.2 Nuclear magnetic resonance (NMR) measurement—Compositions of the QAMs were examined by 1H NMR spectra recorded on a Bruker Avance 300 spectrometer using $CDCl_3$ as the solvent and trimethylsilane as the internal standard.

2.6.3. Elemental analysis—SBG-NS, SBG-NS/KH-570, QAMs, and SBG-QAPMs were compressed to compacted disks of 6 mm in diameter and 1.5 mm thick (n = 3). The measurements were done using the energy dispersive X-ray spectroscopy (EDS) associated with the SEM. For each specimen, ten points were selected randomly for the elemental proportion analysis. The data (n = 3×10 = 30) were recorded and averaged.

2.6.4 Attenuated total reflection Fourier transform infrared (ATR-FTIR) spectroscopy—The ATR-FTIR spectra of SBG-NS, SBG-NS/KH-570, QAMs, and SBG-QAPMs were examined with a Nicolet iS10 FTIR spectrometer (Madison, WI). A range of 500 to 4000 cm^{-1} was scanned at a resolution of 2 cm^{-1}.

2.6.5 Calculation of coupling and grafting ratio—To determine the coupling ratio of KH-570 to SBG-NS and the grafting ratio of QAMs to SBG-NS/KH-570, the weight before (M0, g) modification and the moles (M1, mmol) of KH-570 coupled or QAMs grafted of each sample were measured, and the coupling and grafting ratio was defined as M1/M0 (mmol/g). Three independent tests were performed, and the average and standard deviation were reported.

2.6.6 Stability of SBG-QAPMs—SBG-QAPMs (2.5 g) were added to the PBS solution (50 ml, pH = 7.2) and incubated at 37°C. At the designated time points (1, 3, and 6 months), they were centrifuged, washed twice with PBS, and freeze-dried for 48 h. The residual mass was recorded as M, and the residual percentage mass (Rm) was calculated as Rm = M/2.5 × 100%.

2.7 Evaluation of the antibacterial effect of SBG-QAPMs

The antibacterial effects of SBG-QAPMs against Enterococcus faecalis (E.faecalis, ATCC 29212), *Streptococcus mutans* (*S.mutans*, UA 159), and *Streptococcus sanguis* (*S.sanguis*, ATCC 10556) were determined using the DCT method. Bacteria thawed from their frozen stock were streaked onto Brain Heart Infusion (BHI; Difco, Detroit, MI) agar plates and incubated under anaerobic conditions consisting of 5% CO_2, 85% N_2, and 10% H_2 for 48 h at 37°C. Single colonies were inoculated into 5 ml of BHI broth and incubated anaerobically at 37°C for 48 h. The bacterial suspensions were adjusted spectrophotometrically to approximately 10^8 cells/ml. For the DCT, commercial endodontic products Endomethasone C, AH Plus, and ProRoot MTA (Supporting Information, Table 1) were included as the

controls. Six hundred milligrams of each sealer were prepared according to the manufacturer's instruction. Six hundred milligrams of SBG-QAPMs were prepared with sterilized distilled water. All materials were prepared in aseptic conditions and sterilized with ultraviolet (UV) rays after preparation. These samples were added to 96-well plates and allowed to set for 0 min, 20 min, 24 h, 7 d, 14 d, and 28 d (n = 5, 20 mg/well), respectively. At each designated time point, 10 μL of the bacterial dilution (10^8 cells/ml) was added to the surface of the materials to allow direct contact. They were incubated at 37°C for 1 hour to allow the evaporation of the liquid. Next, BHI broth was added (200 μL/well), and the plates were incubated anaerobically at 37°C for 48 h. The suspensions were diluted in 10-fold steps to 10^{-8}, and 100 μl of each dilution was spread onto BHI agar plates. The plates were then incubated for 48 h at 37°C. The numbers of colony-forming units (CFUs) multiplied by the corresponding dilution ratios represented the number of residual viable bacteria after treatments. In addition, 10 μL of BHI broth and 10 μL of bacterial suspension were added to each empty well and the same treatment was repeated (n = 5). They included the negative control and positive control, respectively. The tests were repeated in triplicate, and the average and standard deviation were reported (n = 15).

2.8 Evaluation of cytocompatibility in vitro

The periodontal ligament stem cells (PDLSCs) used in this study were a gift from Dr. Songtao Shi, University of Pennsylvania. The thawed PDLSCs (passage 2) were cultured in ascorbic acid-free α-modified essential medium (α-MEM) (GIBCO, Invitrogen, Carlsbad, CA) supplemented with 10% fetal bovine serum (FBS) (Invitrogen) and 1% penicillin–streptomycin (Invitrogen) in a humidified incubator with 5% CO_2 at 37°C. The culture medium was changed every other day. The PDLSCs of passages 4–6 were used for all cellular studies. The effects of SBG-HA, Endomethasone C, AH Plus, and ProRoot MTA on the metabolism of the PDLSCs were determined using the LIVE/DEAD staining evaluation and the MTT assay.

For the LIVE/DEAD staining evaluation, freshly mixed samples were stored in α-MEM at 37°C for 24 h to produce the extraction solution. According to the International Organization for Standards (ISO) standard, the ratio between the surface of the sample and the volume of the culture medium was 0.5 cm^2/mL.[18] The collected extraction solution was filtered with a biofilter of 0.2 μm and were used for cell cultures. The PDLSCs were seeded at a density of 5×10^4 cells/well in six-well culture plates. They were allowed to adhere for 24 hr before being replaced with the extraction solution. The experimental groups included: (1) negative control group (cultured with α-MEM and treated with methanol before staining), (2) positive control group (α-MEM), (3) SBG-HA group, (4) Endomethasone C group, (5) AH Plus group, and (6) ProRoot MTA group. Fluorescence staining was performed using a LIVE/DEAD® Viability/Cytotoxicity Assay Kit (Invitrogen, Paisley, UK). The kit consists of two components, Calcein AM and Ethidium homodomer II. Calcein AM is a fluorogenic esterase substrate hydrolysed intracellularly to a green fluorescent product, which is an indicator of live cells. Ethidium homodomer II enters cells through damaged membranes and intercalates with the DNA in the nucleus, emitting a red fluorescent signal. In brief, after 1, 4, and 7 days' incubation, the culture medium (n = 3 in each group) was removed, and the cells were rinsed twice with Dulbecco's phosphate-buffered saline (D-PBS, Gibco). A

staining solution (150 μL) was added to each well. For the negative control group, the cells were treated first with methanol for 30 min before the staining solution was added. The plates were incubated for 30 min at room temperature. After being rinsed with D-PBS, the stained cells were observed using an Eclipse TE2000-U inverted microscope (Nikon Instruments Inc., NY, USA) with a computer-controlled fluorescence microscope light Source (X-Cite® 120PC, Lumen Dynamics Group Inc., Ontario, Canada). For each well, ten representative microscopic fields were selected randomly and recorded.

For the MTT assay, freshly mixed samples were placed into the wells of 96-well culture plates, condensed to disks of approximately 1 mm thick, and sterilized with UV lights. The experimental groups included: (1) control group (uncoated wells), (2) SBG-HA group (coated with SBG-HA), (3) Endomethasone C group (coated with Endomethasone C), (4) AH Plus group (coated with AH Plus), and (5) ProRoot MTA group (coated with ProRoot MTA). The PDLSCs were seeded at a density of 5×10^3 cells per well. After 1, 4, and 7 days' incubation, 20 μL of fresh MTT solution (5 mg/mL; Sigma-Aldrich) was added to the wells of each group (n = 6). The plates were incubated at 37°C for 4 h. The culture media were subsequently removed. The formazan was solubilized in 150 μL per well of dimethyl sulfoxide (DMSO, Sigma), and then the plates were shaken at room temperature for 10 min. The solutions were transferred to a new 96-well plate, and the absorbance was measured at a wavelength of 570 nm using a multi-plate reader (BIO-TEK, Winooski, VT, USA). The data were recorded and averaged. All the experiments were performed in triplicate.

2.9 Evaluation of inflammation in vivo

The animal surgical procedure was approved by the University Committee on the Use and Care of Animals at Texas A&M University College of Dentistry (Protocol # 2016-0071-BCD). A calvarial defect model of Sprague–Dawley rats (8-weeks-old, male, 250–300 g) was used in the current study. SBG-HA, Endomethasone C, AH Plus, and ProRoot MTA were prepared and sterilized as described above. The rats were anesthetized by intraperitoneal injection using a mixture of ketamine (100 mg/kg) and xylazine (10 mg/kg). After the hair was removed, the animal head was fixed in a sterotactic frame (Stoelting Company, Wood Dale, IL, USA) in a prone position. The surgical region was sterilized with iodophor and 70% alcohol. A 1.5 cm-long midsagittal incision was made with a sterile scalpel blade. The soft tissues and periosteum (full thickness flap) were elevated. A 5 mm diameter defect was created in the parietal bone with a trephine drill (Provet SA, Lyssach, Switzerland) under consistent saline cooling. The procedure was conducted cautiously in order to preserve the dura and vessels beneath. After the bleeding was controlled, the freshly prepared materials were carefully implanted on top of the dura. The wound was closed in layers with 5-0 absorbable polyglycolic acid sutures. Fifty animals were divided into five groups: (1) control group (no implants), (2) SBG-HA group (implanted with SBG-HA), (3) Endomethasone C group (implanted with Endomethasone C), (4) AH Plus group (implanted with AH Plus), and (5) ProRoot MTA group (implanted with ProRoot MTA).). In addition, two animals in each group received the same procedures. They were then sacrificed using CO2 asphyxiation, and the X-ray images of the implantation regions were taken and recorded (Fig. S1). At designated time points (2 and 4 weeks), the rats were sacrificed using CO2 asphyxiation. At designated time points (2 and 4 weeks), the rats were sacrificed using

CO2 asphyxiation. Blood samples were immediately collected by heart puncture and centrifuged at 1000 g for 10 min to collect the serum. Serum levels of interleukin 6 (IL6), tumor necrosis factor alpha (TNF-α), and interferon gamma (IFN-γ) were examined using rat ELISA kits (ER3IL6, ER3TNFA, and ERIFNG; ThermoFisher Scientific) according to the manufacturer's instructions. The concentration of each cytokine was calculated with reference to a standard curve constructed using the recombinant rat proteins provided in each kit. All experiments were performed in triplicate.

2.10 Statistical analysis

The quantitative results were presented as mean ± standard deviation (SD). The statistical analyses were performed using the SPSS statistics package for Windows (version 13.0; SPSS Inc., Chicago, IL). For two-sample comparison, an unpaired Student's t-test was applied; for multi-sample comparison, a one-way analysis of variance was applied followed by the Tukey test. The statistical significance level was set at $\alpha = 0.05$.

3 Results

3.1 Syntheses and characterizations of SBG-NS

Silica-based bioactive glass nanospheres were synthesized by a sol-gel process using CTAB as a hydrolysis catalyst. As shown in Fig. 1A, the silica-based bioactive glass samples exhibited regular spherical morphology and did not form any agglomeration. The SBG-NS were mono-dispersed with an average diameter of 181±14 nm (Fig. 1B). The average size of the SBG-NS was controlled by several parameters, including the CTAB concentration, the ratio of reactants, and the reaction time and temperature. For example, the average diameter of the SBG-NS increased from 181 to 307 nm when the CTAB concentration increased from 3.2 to 12.8 mmol/L (Fig. S2).

3.2 Syntheses and characterizations of QAMs

A series of QAMs with different lengths of alkyl chains (n = 3, 9, 16, 18) were successfully synthesized via the addition reaction of tertiary amines with organo-halides. As an example, Fig. 2A shows the 1H NMR spectrum of the HAEMB monomer. The two peaks of 5.52 and 6.03 ppm in the spectrum are attributed to CH_2=C of HAEMB, confirming that the two geminal hydrogens on the carbon of the double bond are exposed to different chemical shift environments and are non-equivalent. As labeled in Fig. 2A, all other peaks were properly assigned to the corresponding hydrogens of the HAEMB monomer.

The ATR-FTIR spectra of the four QAMs (PAEMB, NAEMB, HAEMB, and OAEMB) are shown in Fig. 2B. The peaks at 2925 cm^{-1} and 2850 cm^{-1} are the characteristic peaks of the C-H stretch. The intensity of these two peaks increased as the alkyl chain length of the QAMs increased, confirming the structures of the QAMs.

3.3 Syntheses and characterizations of SBG-QAPMs

The ATR-FTIR spectrum of the SBG-NS shows characteristic absorption bands corresponding to Si-O-Si bonding at 1060 and 798 cm^{-1}, while no apparent peaks are observed at the region of 3000 cm^{-1} to 2800 cm^{-1} or 2000 cm^{-1} to 1500 cm^{-1} (Fig. 3A).

After the coupling reaction of KH-570 to the SBG-NS, new peaks at 1750 cm^{-1} and 1644 cm^{-1} appeared. These two peaks were the characteristic peaks of C=O stretch and C=C stretch, respectively. In addition, two peaks arose at 2925 cm^{-1} and 2850 cm^{-1}, related to the C-H stretch. These results indicated that KH-570 was successfully coupled onto the surface of SBG-NS. When the QAMs were grafted to the SBG-NS/KH-570, the intensity of the C-H peaks stretched at 2925 cm^{-1} and 2850 cm^{-1} increased, consistent with the structure of the alkyl chains of the QAMs. In addition, the intensity of the peak C=C stretch became almost invisible, indicating that the KH-570 was copolymerized with QAMs on the surfaces of the SBG-NS.

The EDS analysis showed that the SBG-NS were composed of elements Si, Ca, P, and O (Fig. 3B). The relative intensity of the peaks indicated the molar ratio of SiO2 : CaO : P2O5 was approximately 82 : 13 : 5. SBG-HA was used as an example to show the elemental changes during the coupling and polymerization processes. No element C was detected in the SBG-NS sample, while a significant amount of element C was found in the SBG-NS/KH-570 and SBG-HA (Fig. 3C). Furthermore, the amount of element C in SBG-HA was significantly higher than that in SBG-NS/KH-570. Meanwhile, the proportion of element Si in the SBG-NS/KH-570 and SBG-HA was significantly lower than that in the SBG-NS. These results confirmed that KH-570 was coupled to the surface of the SBG-NS, and the HAEMB was grafted to the SBG-NS/KH-570.

The morphology and size of the surface-modified SBG-NS were examined using SEM. After the surface modification with QAPMs, the SBG-QAPM showed similar spherical morphology to that of the SBG-NS (Fig. 3D). The average size of the SBG-QAPMs (196±16 nm) was slightly increased compared to the bulk SBG-NS (181±14 nm) (Fig. 3E) ($P < 0.05$).

The coupling ratio of KH-570 to SBG-NS increased when the reaction time increased from 1 h to 24 h (Fig. 4A). However, further increasing the reaction time to 48 h did not have a significant effect on the amount of KH-570 to the SBG-NS. On the other hand, the grafting ratio of QAMs to SBG-NS/KH-570 decreased as the CL of the QAMs increased (Fig. 4B). The stability of the SBG-QAPMs was evaluated in PBS solution at 37°C. The SBG-HA was used as an example of the SBG-QAPMs, and the result is shown in Fig. 4C. There was no significant difference in the average weight of the SBG-HA during the 6-month incubation in PBS ($P > 0.05$), suggesting that the SBG-HA had long-term stability while it was incubated. The other three SBG-QAPMs showed results similar to that of the SBG-HA (data not shown).

3.4 Antibacterial effect of SBG-QAPMs

Three widely used bacteria *E. faecalis, S. mutans, and S. sanguis* were used for the antibacterial test via the DCT method. Fig. 5A–C shows the antibacterial effect of the SBG-HA compared to three representative commercial products (Endomethasone C, AH Plus, and ProRoot MTA) at different treatment times. All these biomaterials provided antibacterial activity within 24 h after they were prepared. Among all three bacteria, Endomethasone C had the strongest antibacterial effect, followed by SBG-HA > AH Plus > ProRoot MTA. However, Endomethasone C, AH Plus, and ProRoot MTA rapidly lost their antibacterial activities after 24 h. In contrast, SBG-HA kept its high antibacterial effect throughout the

28-day experimental time. The other three SBG-QAPMs (SBG-PA, SBG-NA, and SBG-OA) showed an antibacterial curve similar to SBG-HA against *E.faecalis, S.mutans,* and *S.sanguis* (Fig. 5D, E, and F). Among the SBG-QAPMs, the antibacterial effect was SBG-HA > SBG-OA > SBG-NA > SBG-PA. Therefore, SBG-HA was selected for the following biocompatibility and in vivo inflammation evaluations.

3.5 Evaluation of SBG-QAPMs cytocompatibility *in vitro*

The cytocompatibility of the SBG-HA was evaluated using LIVE/DEAD staining and compared with Endomethasone C, AH Plus, and ProRoot MTA (Fig. 6). Throughout the entire culture period of 7 days, almost all the PDLSC cells in the SBG-HA and ProRoot MTA groups were green and exhibited the same morphology as that of the positive control, indicating that the SBG-HA and ProRoot MTA had high cytocompatibility. In the AH Plus group, a few green cells were observed at day 1. The cells became oval, and their density dramatically decreased at day 4. At day 7, no living cells were detected in the AH Plus group. No viable cells were observed at all test time points in the Endomethasone C group, due to the high cytotoxicity of Endomethasone C.

The MTT assay further confirmed the results of the LIVE/DEAD staining evaluation. As shown in Fig. 7, the proliferation rate of the PDLSCs in the Endomethasone C group was significantly lower than that in all the other groups at all time points ($P < 0.001$). The cell number in the SBG-HA and ProRoot MTA groups was significantly higher than that in the AH Plus at days 4 and 7 ($P < 0.001$). In addition, there were no significant differences in PDLSC proliferation between the SBG-HA, ProRoot MTA, and the positive control group from days 1 to 7. These results indicated that the SBG-HA had high cytocompatibility.

3.6 Evaluation of inflammation *in vivo*

The systemic inflammation caused by implanting the SBG-HA in vivo was also evaluated and compared with Endomethasone C, AH Plus, and ProRoot MTA (Fig. 8). After these biomaterials had been implanted for 2 weeks, the serum level of IFN-γ was SBG-HA < ProRoot MTA, Endomethasone C < AH Plus (Fig. 8A). At 4 weeks, the IFN-γ in the SBG-HA decreased to the level of the blank control group, while it was still relatively high in the other three commercial prodcts (Fig. 8A). Similarly, the levels of IL-6 and TNF-α at 2 and 4 weeks were SBG-HA < ProRoot MTA, Endomethasone C < AH Plus (Fig. 8B&8C). These results indicated that SBG-HA had the least systemic inflammation compared with the ProRoot MTA, Endomethasone C, and AH Plus.

4 Discussion

In this study, we developed a novel type of quaternized mono-dispersed bioactive glass-based SBG-QAPMs as substrates for long-term antibacterial endodontic sealers and tested their antibacterial effect, cytocompatibility *in vitro*, and their potential systemic inflammation when implanted *in vivo*. Our results indicated that the SBG-QAPMs had the strongest long-term antibacterial activity, the best cytocompatibility, and the lowest systemic inflammation compared to the three commercial products ProRoot MTA, Endomethasone C and AH Plus.

While SBG nanoparticles are readily synthesized via a sol-gel process, controlling the spherical size and their distribution, as well as preventing cohesion, is difficult.[19] Different structure-directing agents were tested to obtain SBG with controlled size and distribution.[29] In this study, we chose CTAB to act as a templating agent to prevent the SBG-NS from sticking together. Moreover, the addition of CTAB into the synthesis route controlled the formation of mono-dispersed SBG-NS under our synthetic conditions. Therefore, our approach to the addition of CTAB effectively solved the problems of the severe agglomeration and irregularity that accompany the SBG nanoparticles fabricated with the conventional sol-gel method. The SBG-NS compositions (SiO_2/CaO = 82/13) were different from the originally designed oxide content (SiO_2/CaO = 84/16), which suggests that some calcium ions were not incorporated into the SBG-NS and were removed during the washing step. Similar results were reported for the preparation of the SBG nanospheres using the standard and modified Stöber methods.[30]

A two-step approach was developed for this study to covalently graft antibacterial quaternary ammonium salts onto the surface of SBG-NS. First, KH-570 was reacted with the silanol groups to introduce C=C double bonds on the surfaces of SBG-NS. Next, QAMs with different lengths of alkyl chains were grafted on the surface of SBG-NS/KH-570 by copolymerization with the KH-570. The intensity of peaks at 2925 cm^{-1} and 2850 cm^{-1} related to the C-H stretch increased after copolymerization, confirming that the QAPMs were covalently grafted onto the surfaces of the SBG-NS (Fig. 3). The coupling ratio of KH-570 to the SBG-NS was controlled by the reaction time. However, the amount of KH-570 did not increase after 24 h, suggesting that the available surfaces of the SBG-NS were coupled to KH-570. Meanwhile, the grafting ratio of QAMs to SBG-NS/KH-570 decreased as the CL of the QAMs increased. The decrease in the grafting ratio with the alkyl chain length of the QAMs is attributed to the steric hindrance effect.

Due to the complication of the human root canal system, conventional chemo-mechanical techniques cannot completely eliminate infections within the canal.[7,8,31] Mechanical debridement can only eliminate bacteria and necrotic tissues located in the main root canal. Root canal irrigation can reach some areas (e.g., the dentinal tubule) beyond the scope of the mechanical debridement to improve the disinfection efficacy. However, even sodium hypochlorite, the most effective root canal irrigant currently used, can penetrate only to a depth of approximately 130 μm into dentinal tubules, leaving bacteria in the deeper layers unaffected.[31,32] In addition, bacteria located in areas such as accessory canals, anastomoses, and fins, cannot be eliminated by either mechanical debridement or root canal irrigation.[33] Therefore, an endodontic sealer should have antibacterial activity to eliminate or inhibit the growth of residual bacteria that are untouched by the chemo-mechanical procedures. Although a few endodontic sealers were reported could present a certain antibacterial effect up to 30 days and even a longer time, the majority of current sealers have only short-term antibacterial activity[12–14], which results from the release of antibacterial components in the sealer. For example, ZnOE-based sealers present a strong antibacterial effect against various bacteria including *E.faecalis, Staphylococcus aureus,* and *S.mutans*[34–36] when the sealing components are freshly mixed. However, such antibacterial activity decreases rapidly due to the consumption of the free eugenol and ZnO in the sealer and eventually disappears when the sealer is set.

To provide a long-term antibacterial activity in a sealer, we synthesized a series of antibacterial QAMs and covalently grafted them onto the surfaces of the SBG-NS. In this study, the antibacterial effect was examined using the DCT, which is a quantitative method that has been proven to be reproducible. The DCT can reflect the antibacterial effect of an endodontic sealer by mimicking their contact with bacteria in the clinic.[37] *E.faecalis*, *S.mutans*, and *S.sanguis* were selected as test microorganisms because they have been reported to frequently be the persistent pathogens associated with refractory periapical periodontitis.[38] As we predicted, the SBG-QAPMs showed a consistently effective antibacterial effect against *E.faecalis*, *S.mutans*, and *S.sanguis* during the study period (from freshly mixed to 28 d after preparation). However, only fresh samples (within 24 h after preparation) of Endomethasone C, AH Plus, and ProRoot MTA showed an effective antibacterial effect against the test microorganisms. None of their set samples (7, 21, and 28 d after preparation) showed an acceptable antibacterial effect compared with the control group. Similar results were reported that QAPMs presented a consistent antibacterial effect against both gram-negative and gram-positive bacteria,[39] and their bactericidal activity depends on the positive charges on the molecular chain.[17] It is generally considered that the electrostatic interactions between the positively-charged quaternary ammonium group of the QAMs and the negatively-charged bacteria cell membrane disrupt the construction, leading to leakage of cytoplasmic material and cellular lysis.[40] The polymerization of QAMs on the surface of SBG-NS resulted in a high density of NH_4^+ on the surfaces of the SBG-QAPMs, therefore conferring a strong antibacterial effect on the SBG-QAPMs. In addition, the bactericidal activities of the SBG-QAPMs were affected by the CL of the QAMs, and the CL=16 (corresponding to SBG-HA) had the highest antibacterial effect. Similar results were reported that the antibacterial activities increased when the CL was increased from 3 to 16, and then reduced as the CL was further increased.[41,42] The high bactericidal activity of the CL=16 may be due to the fact that both the outer and the plasma membrane lipid bilayers of the bacteria can accommodate the entire hydrocarbon chain length of the QAMs and that longer hydrophobic chains will have a greater hydrophobic effect.[43]

Endodontic sealers are supposed to remain within the root canal system. However, it is possible that they might over-extrude into the periapical areas.[44] Direct contact and degradation of endodontic sealers over time can cause cytotoxic damage to cells and tissues and trigger chronic inflammation, endangering the success of endodontic treatment.[45,46] Thus, an endodontic sealer should show good biocompatibility to periapical tissues. In this work, a cytotoxicity evaluation of the test materials was performed when they were freshly mixed, consistent with the clinical procedure of inserting endodontic sealers into a root canal system in a freshly mixed and incompletely set stage. It was reported that endodontic sealers are the most cytotoxic when they are freshly mixed.[44,47] While several cell types have been employed to investigate the cytotoxicity of endodontic sealers, including osteoblasts, mouse fibroblasts, and human fibroblasts, we selected human periodontal ligament fibroblasts due to the close relationship of endodontic sealers and periapical tissues.[47,48]

Using SBG-HA as an example, we compared the cytocompatibility and biocompatibility of SBG-QAPMs with three commercial endodontic products (Endomethasone C, AH Plus, and ProRoot MTA). The *in vitro* evaluation showed that the SBG-HA had favorable cytocompatibility similar to that of ProRoot MTA and was superior to that of

Endomethasone C and AH Plus. Endomethasone C is a ZnOE-based sealer, and the cytotoxicity of ZnOE-based sealers results from the release of eugenol.[49] The released eugenol has severe cytotoxicity on various cell types including periodontal ligament (PDL) cells.[47,48] As an epoxy-resin-based sealer, fresh AH Plus has moderate to severe cytotoxicity both *in vitro* and *in vivo*.[45,47,50] Its cytotoxicity is likely associated with the release of a small amount of formaldehyde and/or bisphenol-A diglycidyl ether from the resin.[45,50]

It is well-known that bioactive glasses have excellent biocompatibility. The SiO_2-CaO glass with a range of 50–90 mol% SiO_2 in the system was bioactive and formed an apatite layer in simulated body fluid.[51] The bioactivity of the sol-gel bioglass nanoparticles with high silica contents is related to the broad distribution of the bonding network between the oxygen and silicon atoms.[52] The SBG was able to enhance the odontogenic differentiation of human dental pulp stem cells and stimulate the growth and osteogenic differentiation of the human primary osteoblasts.[16,53] Our results confirmed that the SBG-QAPMs retained high bioactivity, similar to other bioactive glasses.

An *in vivo* inflammation test was further performed to compare the biocompatibility of SBG-QAPMs with the three commercial products. Among all those four materials, the SBG-HA always induced the lowest levels of inflammatory factors (IFN-γ, IL-6 and TNF-α) in the blood after being implanted for 2 and 4 weeks. In fact, the level of the inflammatory factors in SBG-HA decreased to that of the blank control group at 4 weeks. These results showed that the SBG-HA had the lowest systemic inflammation effect compared to ProRoot MTA, Endomethasone C, and AH Plus.

An endodontic sealer ideally should be water insoluble so that to have a good sealing capability; however, most of the commercial sealers lose a small amount of weight when immersed in aqueous solution for certain periods of time.[54] For example, it was reported that ZnOE-based sealers had a water solubility of 1–7% after being stored at 37°C and 95% humidity for 24 h.[55] An epoxy-based sealer (AH 26) stored in water for 28 days had a weight loss of approximately 2.6%.[54] MTA-based sealers were reported to have a stability similar to that of epoxy-resin-based sealers.[56] Therefore, to develop an endodontic sealer, the SBG-QAPMs should have a good stability in aqueous solution. In the present study, when the SBG-QAPMs were immersed in PBS for a 6-month period of time, there was no significant difference in the average weight (Fig. 4). This indicated that the SBG-QAPMs had high stability in aqueous solution, and might have an excellent sealing capability when they are used for endodontic sealers. The primary goal of this study was to synthesize, characterize, and test the potential of the SBG-QAPMs as a main substrate for a new antibacterial endodontic sealer. To develop an endodontic sealer, more components (e.g. matrix and additives) need to be included in the SBG-QAPMs, and the investigation on their properties (e.g. setting time, flowability, and volume shrinkage) will be explored in our future experiments.

5 Conclusion

A three-step approach was developed to synthesize a novel type of quaternized mono-dispersed bioactive SBG-QAPMs. These SBG-QAPMs showed a consistently effective,

long-term antibacterial effect, favorable cytocompatibility and biocompatibility, and excellent stability in aqueous solution. Therefore, the SBG-QAPMs are promising substrates for the development of long-term antibacterial endodontic sealers.

Supplementary Material

Refer to Web version on PubMed Central for supplementary material.

Acknowledgments

Xiaogang Cheng and Tiejun Qu contributed equally to this work. It was supported by NIH/NIDCR grant R01DE024979 to X. Liu and the National Natural Science Foundation of China (No. 31271048) and the Innovation Team of the Ministry of Education (No. IRT13051) to Q. Yu. The authors would like to thank Dr. Songtao Shi for providing the PDLSCs, and Jeanne Santa Cruz for her assistance with the editing of this article.

References

1. Kureishi A, Chow A. Infec. Dis. Clin. North Am. 1988; 2:163. [PubMed: 3074106]
2. Tao L, Herzberg MC. Method Enzymol. 1998; 310:109.
3. Genco R, Offenbacher S, Beck J. J. Am. Dent. Assoc. 2002; 133:14S. [PubMed: 12085720]
4. Kaur A, Shah N, Logani A, Mishra N. J. Conserv. Dent. 2015; 18:83. [PubMed: 25829682]
5. Tyagi S, Mishra P, Tyagi P. European J. Gen. Dent. 2013; 2:199.
6. Zehnder M. J. Endod. 2006; 32:389. [PubMed: 16631834]
7. Nair P, Henry S, Cano V, Vera J. Oral Surg. Oral Med. Oral Pathol. Oral Radiol. Endo. 2005; 99:231.
8. Sjogren U, Figdor D, Persson S, Sundqvist G. Int. Endod. J. 1997; 30:297. [PubMed: 9477818]
9. Hume WR. J. Am. Dent. Assoc. 1986; 113:789. [PubMed: 3537057]
10. Leonardo MR, da Silva LAB, Tanomaru Filho M, da Silva RS. Oral Med. Oral Pathol. Oral Radiol. Endo. 1999; 88:221.
11. Kreth J, Kim D, Nguyen M, Hsiao G, Mito R, Kang M, Chugal N, Shi W. Open Dent. J. 2008; 2:18. [PubMed: 19088878]
12. Wang Z, Shen Y, Haapasalo M. J. Endod. 2014; 40:505. [PubMed: 24666900]
13. Du T, Wang Z, Shen Y, Ma J, Cao Y, Haapasalo M. J. Endod. 2015; 41:1294. [PubMed: 26092772]
14. Sagsen B, Er O, Esel D, Yagmur G, Altintop Y. J. Contemp. Dent. Pract. 2009; 10:35.
15. Zhou H, Du T, Shen Y, Wang Z, Zheng Y, Haapasalo M. J. Endod. 2015; 41:56. [PubMed: 25442721]
16. Qu T, Liu X. J. Mater. Chem. B. 2013; 1:4764.
17. Buffet-Bataillon S, Tattevin P, Bonnaure-Mallet M, Jolivet-Gougeon A. Inter. J. Antimicro. Ag. 2012; 39:381.
18. Gorduysus M, Avcu N, Gorduysus O, Pekel A, Baran Y, Avcu F, Ural AU. J. Endod. 2007; 33:1450. [PubMed: 18037057]
19. Jones JR. Acta Biomater. 2013; 9:4457. [PubMed: 22922331]
20. Poggio C, Lombardini M, Colombo M, Dagna A, Saino E, Arciola CR, Visai L. Inter. J. Artif. Organs. 2011; 34:908.
21. Heyder M, Kranz S, Völpel A, Pfister W, Watts DC, Jandt KD, Sigusch BW. Dent. Mater. 2013; 29:542. [PubMed: 23523285]
22. Sharma D, Grover R, Pinnameneni PS, Dey S, Raju PR. J. Inter. Oral Health. 2014; 6:90.
23. Baer J, Maki JS. J. Endod. 2010; 3:1170.
24. Hoelscher AA, Bahcall JK, Maki JS. J Endod. 2006; 32:145. [PubMed: 16427465]
25. Kishen A, Shi Z, Shrestha A, Neoh KG. J. Endod. 2008; 34:1515. [PubMed: 19026885]

26. Farmakis ETR, Kontakiotis EG, Tseleni-Kotsovili A, Tsatsas VG. J. Investig. Clin. Dent. 2012; 3:271.
27. Prestegaard H, Portenier I, Ørstavik D, Kayaoglu G, Haapasalo M, Endal U. Acta Odontol. Scand. 2014; 72:970. [PubMed: 25005627]
28. Willershausen I, Callaway A, Briseno B, Willershausen B. Head Face Med. 2011; 7:15. [PubMed: 21831282]
29. Wu C, Chang J. Interfce Focus. 2012; 2:292.
30. Lukowiak A, Lao J, Lacroix J, Nedelec J-M. Chem. Commun. 2013; 49:6620.
31. Cheng X, Guan S, Lu H, Zhao C, Chen X, Li N, Bai Q, Tian Y, Yu Q. Laser Surg. Med. 2012; 44:824.
32. Berutti E, Marini R, Angeretti A. J. Endod. 1997; 23:725. [PubMed: 9487845]
33. Bystrom A, Sundqvist G. Eur. J. Oral Sci. 1981; 89:321.
34. Grossman L. J. Endod. 1980; 6:594. [PubMed: 6778948]
35. Sipert C, Hussne R, Nishiyama C, Torres S. Int. Endod. J. 2005; 38:539. [PubMed: 16011772]
36. Queiroz, AMd, Nelson Filho, P., Silva, LABd, Assed, S., Silva, RABd, Ito, IY. Braz. Dent. J. 2009; 20:290. [PubMed: 20069251]
37. Pizzo G, Giammanco GM, Cumbo E, Nicolosi G, Gallina G. J. Dent. 2006; 34:35. [PubMed: 15907357]
38. Sundqvist G, Figdor D, Persson S, Sjogren U. Oral Surg. Oral Med. Oral Pathol. Oral Radiol. Endo. 1998; 85:86.
39. Mondrzyk A, Fischer J, Ritter H. Polym. Int. 2014; 63:1192.
40. Gottenbos B, van der Mei HC, Klatter F, Nieuwenhuis P, Busscher HJ. Biomaterials. 2012; 23:1417.
41. Zhou H, Li F, Weir MD, Xu HHK. J. Dent. 2013; 41:1122. [PubMed: 23948394]
42. He JW, Soderling E, Osterblad M, Vallittu PK, Lassila LVJ. Molecules. 2011; 16:9755. [PubMed: 22113583]
43. Lindstedt M, Allenmark S, Thompson RA, Edebo L. Antimicrob. Agents Chemother. 1990; 34:1949. [PubMed: 2291660]
44. Camps J, About I. J. Endod. 2003; 29:583. [PubMed: 14503832]
45. Lodienė G, Morisbak E, Bruzell E, Ørstavik D. Int. Endod. J. 2008; 41:72. [PubMed: 17931390]
46. Lopez-Lopez J, Estrugo-Devesa A, Jane-Salas E, Segura-Egea J. Int. Endod. J. 2012; 45:98. [PubMed: 21883296]
47. Schwarze T, Fiedler I, Leyhausen G, Geurtsen W. J. Endod. 2002; 28:784. [PubMed: 12470025]
48. Huang FM, Tai KW, Chou MY, Chang YC. Int. Endod. J. 2002; 35:153. [PubMed: 11843970]
49. Linqvist L, Otteskog P. J. Dent. Res. 1981; 89:552.
50. Silva, EJNLd, Santos, CC., Zaia, AA. J. Appl. Oral Sci. 2013; 21:43. [PubMed: 23559111]
51. Martinez A, Izquierdo-Barba I, Vallet-Regi M. Chem. Mater. 2000; 12:3080.
52. Labbaf S, Tsigkou O, Mueller KH, Stevens MM, Porter AE, Jones JR. Biomaterials. 2011; 32:1010. [PubMed: 21071080]
53. Xynos I, Hukkanen M, Batten J, Buttery L, Hench L, Polak J. Calcif. Tiss. Int. 2000; 67:321.
54. Schafer E, Zandbiglari T. Int. Endo. J. 2003; 36:660.
55. Camps J, Pommel L, Bukiet F, About I. Dent. Mater. 2004; 20:915. [PubMed: 15501319]
56. Gomes-Filho JE, Watanabe S, Bernabe PFE, de Moraes Costa MT. J. Endod. 2009; 35:256. [PubMed: 19166785]

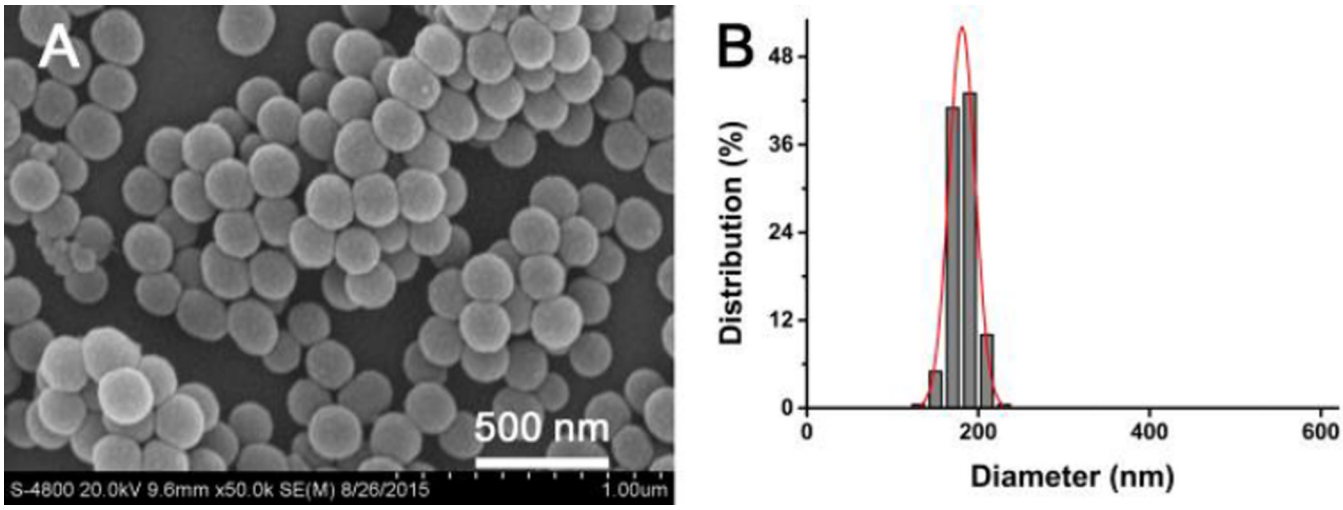

Fig. 1.

Characterizations of SBG-NS. (A) SEM image of SBG-NS, showing that the SBG-NS were spherical and mono-dispersed. (B) Size distribution of the SBG-NS.

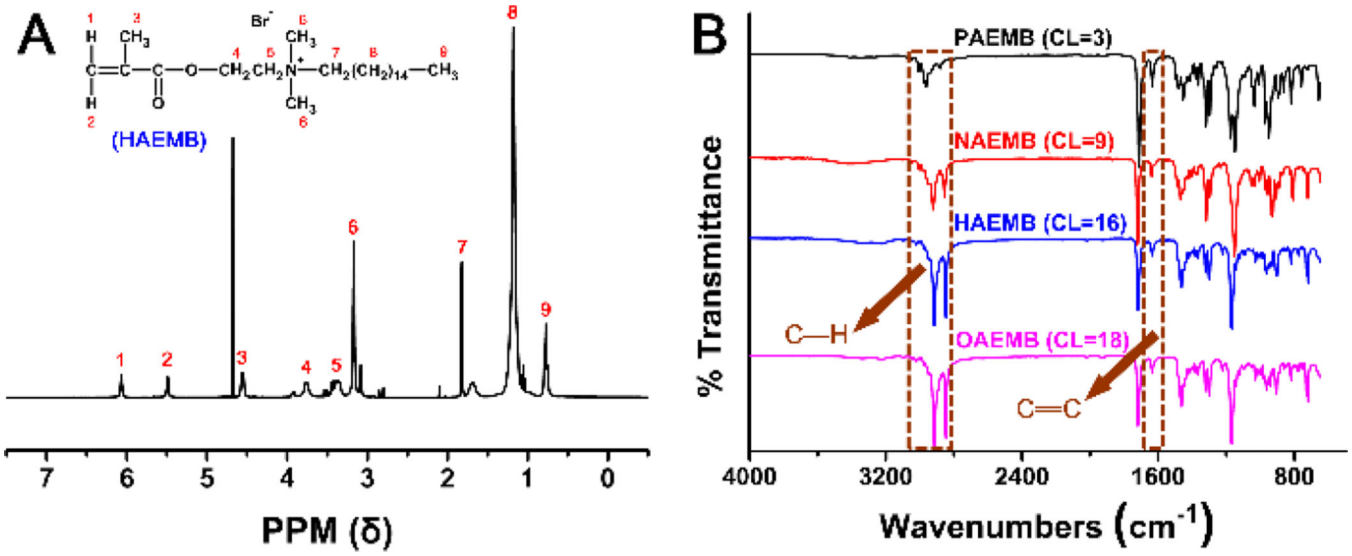

Fig. 2.

Characterizations of the QAMs. (A) ^{1}H NMR spectrum of the HAEMB monomer. (B) ATR-FTIR spectra of the four QAMs (PAEMB, NAEMB, HAEMB, and OAEMB).

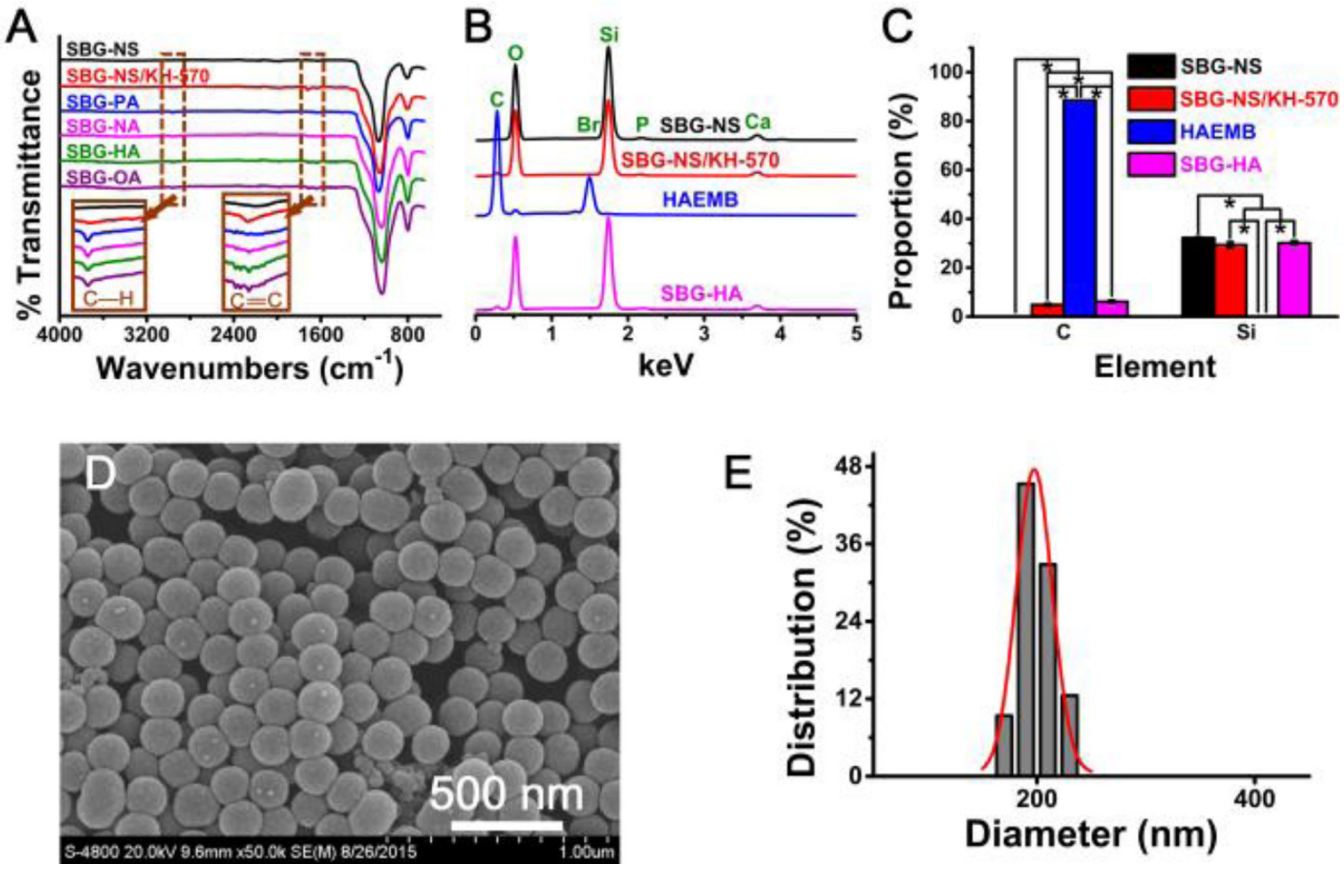

Fig. 3.

(A) The ATR-FTIR spectra of SBG-NS, SBG-NS/KH-570, and SBG-QAPMs (SBG-PA, SBG-NA, SBG-HA, and SBG-OA). (B) EDS spectra of the SBG-NS, SBG-NS/KH-570, HAEMB, and SBG-HA. (C) The elemental analyses of SBG-NS, SBG-NS/KH-570, and SBG-QAPMs. **P < 0.01, ***P < 0.001. (D) SEM image of SBG-HA. Scale bar = 500 nm. (E) Size distribution of the SBG-HA.

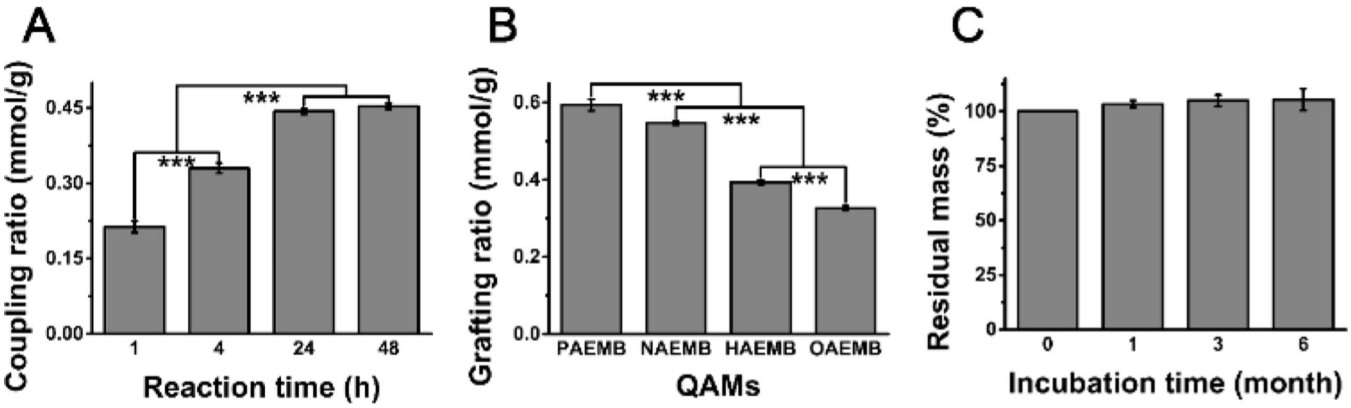

Fig. 4.

(A) The coupling ratio of KH-570 to SBG-NS. (B) The grafting ratio of QAMs (PAEMB, NAEMB, HAEMB, and OAEMB) to SBG-NS/KH-570 (B). ***P < 0.001. (C) The stability of the SBG-QAPMs in PBS solution.

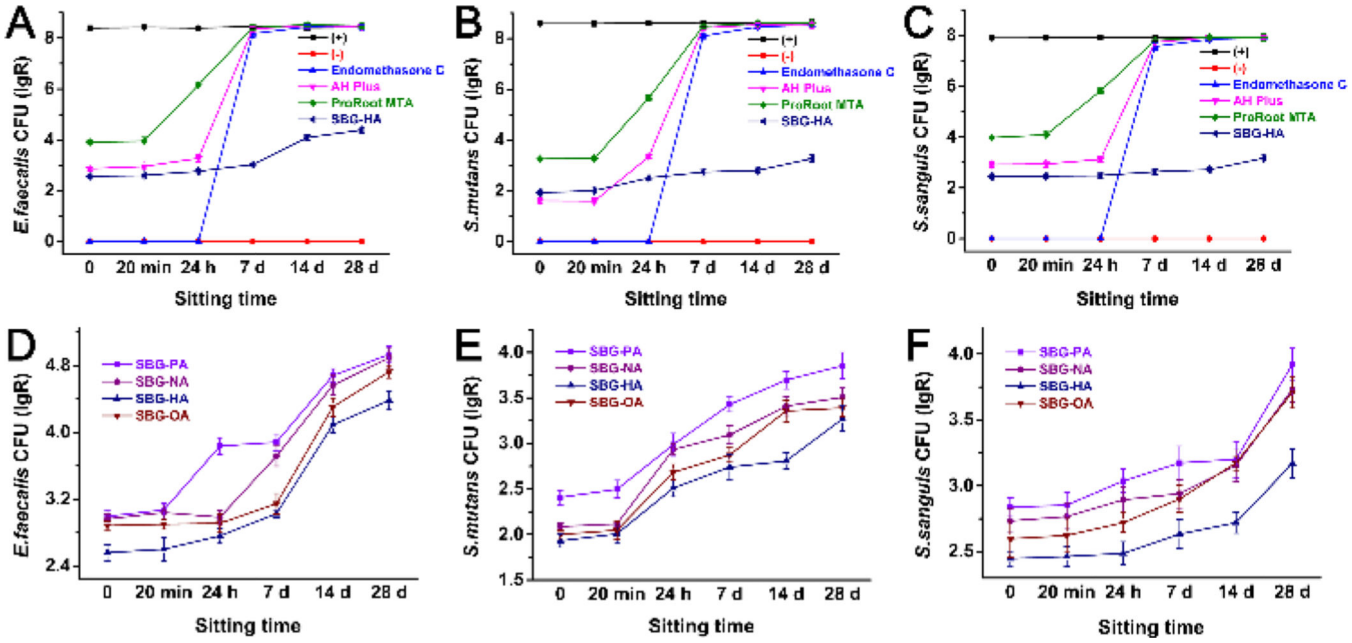

Fig. 5.

Antibacterial effect of the SBG-QAPMs (SBG-PA, SBG-NA, SBG-HA, and SBG-OA) and three commercial endodontic products (Endomethasone C, AH Plus, and ProRoot MTA) against the E. faecalis, S. mutans, and S. sanguis. (+), bacterial suspension only; (−), culture medium only.

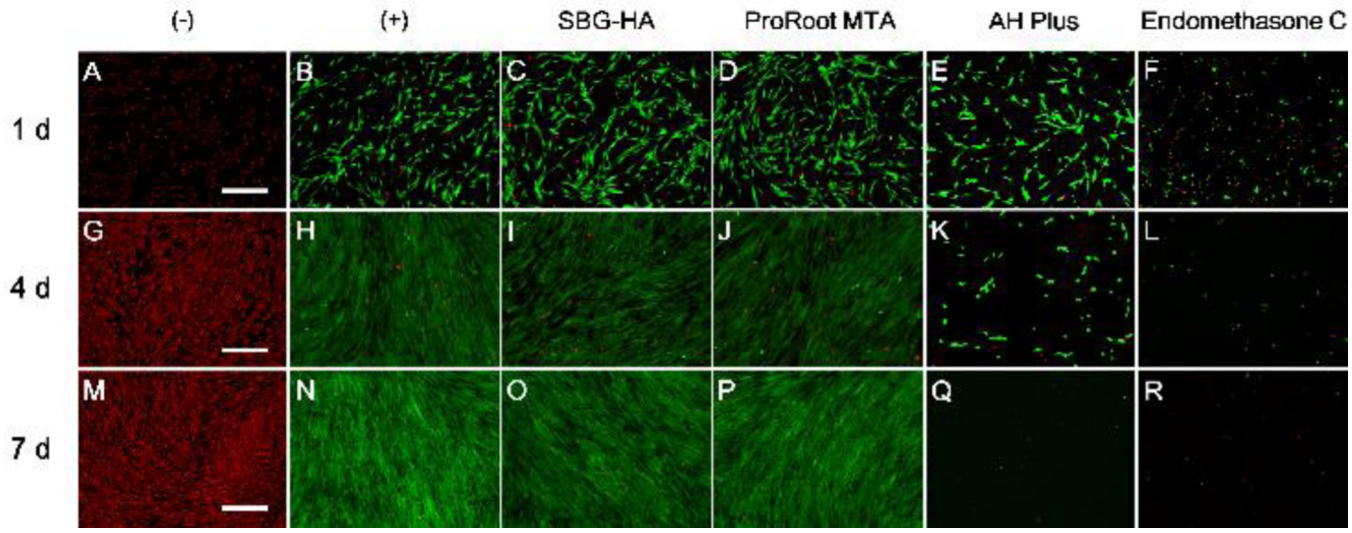

Fig. 6.

In vitro cytocompatibility (LIVE/DEAD staining) of the SBG-HA to the PDLSCs compared with Endomethasone C, AH Plus, and ProRoot MTA. The green fluorescence represented viable cells while the red fluorescence represented dead cells. Scale bar = 500 μm.

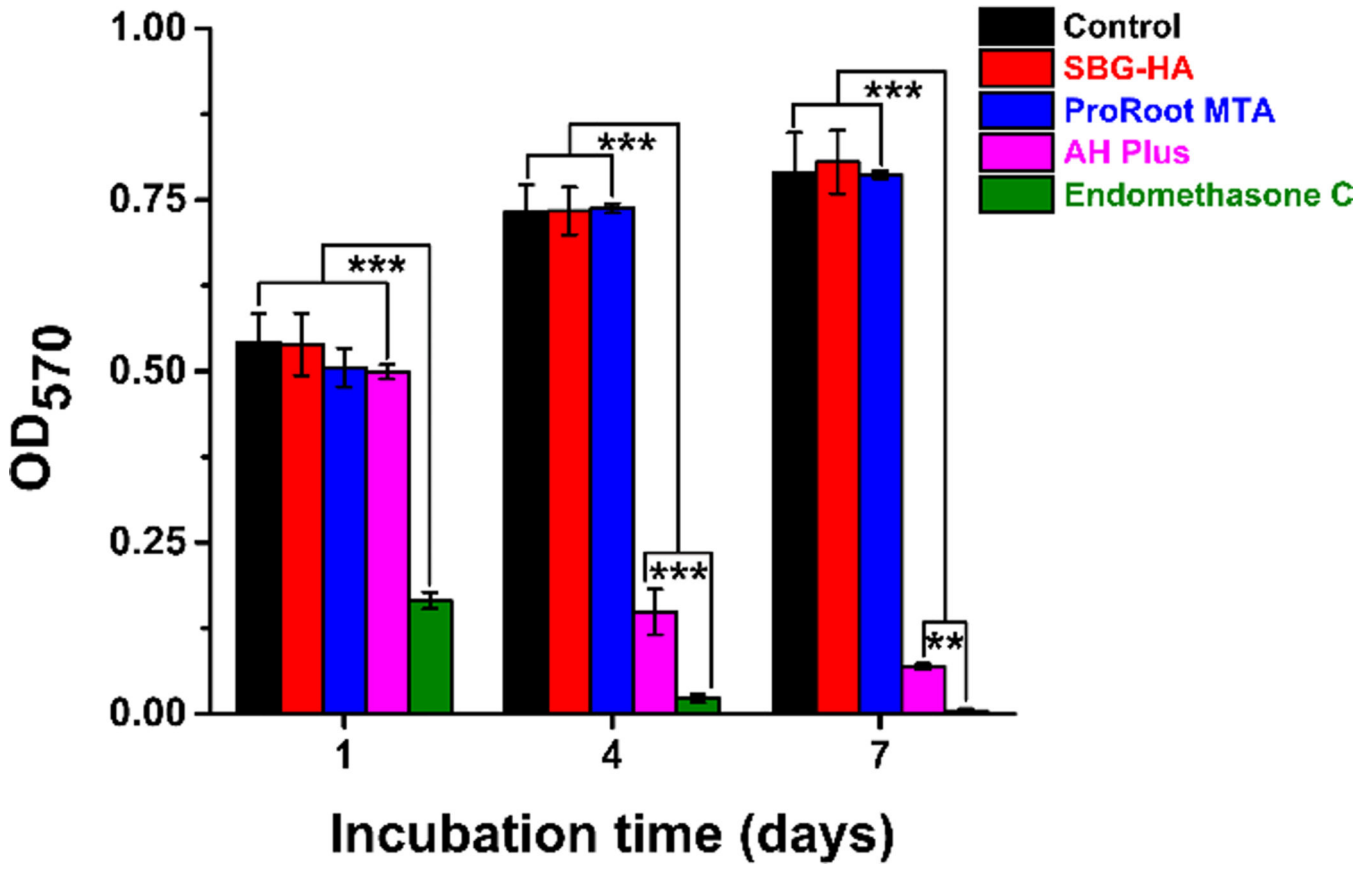

Fig. 7.

MTT assay of the SBG-HA and Endomethasone C, AH Plus, and ProRoot MTA. **P < 0.01, ***P < 0.001.

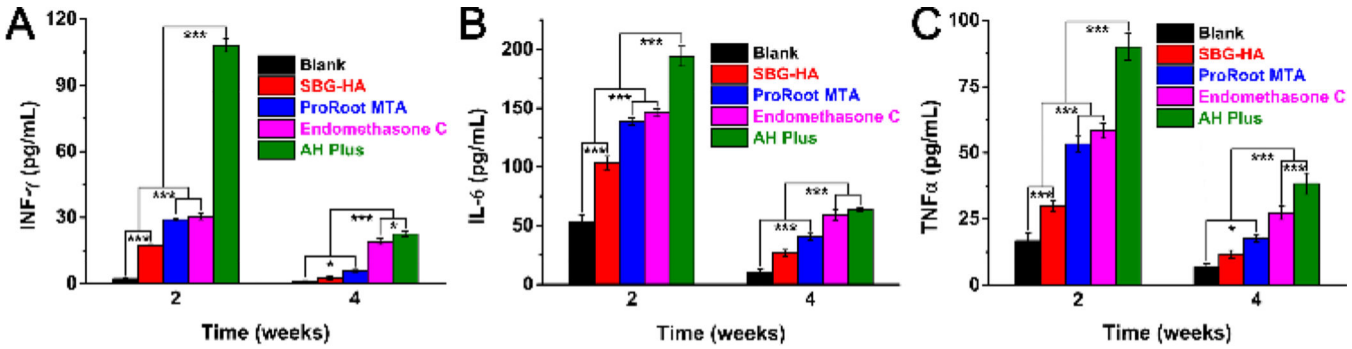

Fig. 8.

In vivo inflammatory reaction of the SBG-HA, Endomethasone C, AH Plus, and ProRootMTA after being implanted in a calvarial defect of SD rats for 2 and 4 weeks. *P < 0.05, **P < 0.01, ***P < 0.001.

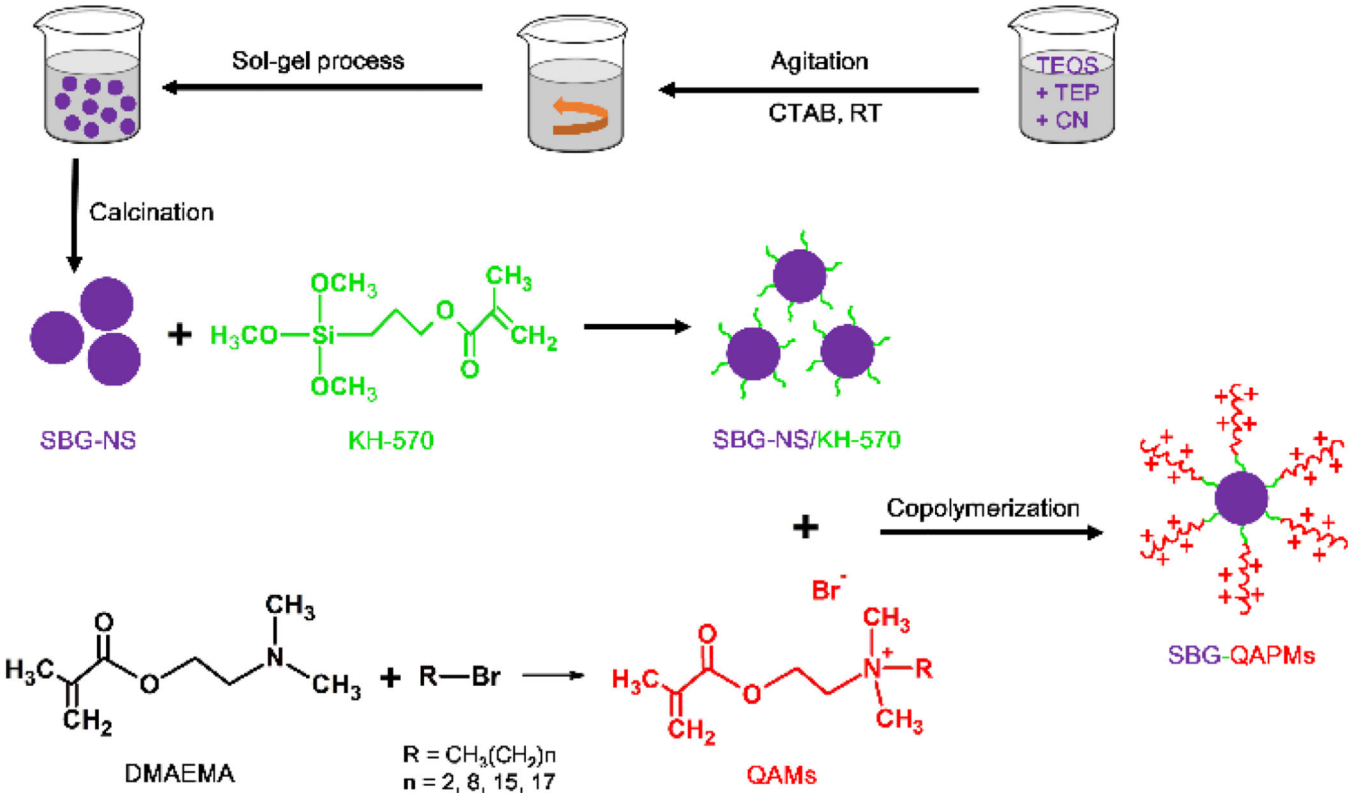

Scheme 1.
Schematic diagram of synthesizing SBG-QAPMs.